



# Mid-infrared optical parametric chirped-pulse amplifier at 50 W and 38 fs pumped by a high-power Yb-InnoSlab platform

JAN HEYE BUSS,<sup>1</sup> SEBASTIAN STAROSIELEC,<sup>1</sup> MICHAEL SCHULZ,<sup>1</sup>  
ROBERT RIEDEL,<sup>1</sup> FILIPPO CAMPI,<sup>2</sup> CARL STEFAN LEHMANN,<sup>2</sup>  
STEFAN WITTE,<sup>2,3</sup>  AND PETER M. KRAUS<sup>2,3,\*</sup> 

<sup>1</sup>Class 5 Photonics GmbH, Notkestraße 85, 22607 Hamburg, Germany

<sup>2</sup>Advanced Research Center for Nanolithography, Science Park 106, 1098 XG Amsterdam, The Netherlands

<sup>3</sup>LaserLab, Department of Physics and Astronomy, Vrije Universiteit Amsterdam, De Boelelaan 1105, 1081 HV Amsterdam, The Netherlands

\*kraus@arcnl.nl

**Abstract:** High-power Yb:InnoSlab lasers are proliferating into multiple modern application areas of laser physics ranging from plasma physics and nanolithography to driving optical parametric amplifiers for high-harmonic generation and attosecond science. Here, we present, the layout, design and first results of an optical parametric chirped-pulse amplifier system pumped by a kW-level average power Yb-InnoSlab laser. We describe the layout and concepts of the pump lasers, with particular attention to the specific design principles required for our application. In the current configuration, the pump laser delivers up to 933 W, 18.7 mJ, 1.2 ps pulses at 50 kHz repetition rate. In a first attempt this has generated above 70 W average power at 2  $\mu\text{m}$  via parametric amplification. Chirped-mirror compression resulted in mJ-level pulses at 50 W and 38-fs pulse duration (5.7 cycles at 2  $\mu\text{m}$ ).

© 2024 Optica Publishing Group under the terms of the [Optica Open Access Publishing Agreement](#)

## 1. Introduction

High-average-power ultrafast lasers find myriad applications in industrial manufacturing, ranging from laser-produced plasma sources for extreme-ultraviolet lithography [1,2], as pump laser for table-top extreme-ultraviolet and soft-X-ray lasers [3,4], and as pump laser for optical parametric chirped-pulse amplifiers (OPCPAs) [5–7].

In particular, OPCPAs profit from picosecond-duration pump lasers, which is beneficial for temporal contrast and allows for simple compression schemes such as chirped-mirror compressors. This rules out established high-power platforms based on Q-switching such as CO<sub>2</sub> lasers. Yb:YAG as a gain medium combines low defect levels with a broad gain bandwidth that supports ultrashort pulses with high efficiency and favorable thermal properties, making it a preeminent choice for OPCPA pump lasers [8,9] - either in a thin disk configuration [10,11], as cryogenically cooled rods [12], or as InnoSlab medium [13–15].

Here, we highlight two particular (potential) use cases: First, InnoSlab laser have become workhorses for operating in the mJ pulse energy and tens to hundreds of kHz repetition rate range, where a particularly strong pull comes from the ever increasing demands from the microelectronic industry. A particular use case of InnoSlab could be assisting in driving EUV tin-plasma lithography sources, the drive lasers of which may become solid-state lasers due to their improved energy efficiency compared to the industry standard of CO<sub>2</sub> lasers [1].

Second, InnoSlab laser are a particularly suitable choice for OPCPAs: The Yb transitions provide a favorable pumping wavelength with attainable (sub-)ps pulse duration for conversion into the mid-infrared, which is an often sought target wavelength for OPCPAs [8,16]. The few-pass geometry of InnoSlab lasers provides an intrinsically low accumulation of nonlinear

phase shift through the amplification chain, which is commonly quantified as B-integral. This is particularly favorable compared to regeneratively amplified systems, which are often used in thin-disk lasers. These systems employ a cavity-based design with Pockels cells or other pulse picking elements, through which the pulses are transmitted in every amplification round trip.

A number of OPCPAs driven by various pump lasers have been demonstrated in literature, and a recent summary of available OPCPA systems can be found in Refs. [17,18], both of which contain this work as disseminated in a previous conference paper [17].

We particularly note a 27 W 2.1  $\mu\text{m}$  OPCPA system at 10 kHz [19], a 49 W carrier-envelope-phase-stable few-cycle 2.1  $\mu\text{m}$  OPCPA at 10 kHz [18], a carrier-envelope-phase-stable, 1.2 mJ, 1.5 cycle laser system at 2.1  $\mu\text{m}$  [20], a 100 W high-repetition-rate near-infrared OPCPA [21], as well as longer wavelength systems such as a few-cycle OPCPA system at 3.2  $\mu\text{m}$  [22], an OPCPA at 3  $\mu\text{m}$  [23] and a dual beam 43 W, 1.55  $\mu\text{m}$  and 12.5 W, 3.1  $\mu\text{m}$  100 kHz OPCPA [24].

Here, we present the outline and status of a 50-kHz OPCPA system at 2  $\mu\text{m}$  pumped by a kW-level Yb:InnoSlab laser. We particularly sought out a design that gives a very high average power above 50 W and pulse energies above 1 mJ, while at the same time keeping the pulse duration close to 5 optical cycles. In particular, this configuration allows for mJ level output, which is desirable for subsequent use in high-harmonic generation while retaining the highest possible repetition rate. Our OPCPA design can even operate in the multi-mJ energy range. This property and all other specifications are chosen as they are ideally suited for our applications in attosecond science [25] and coherent soft-X-ray imaging at photon energies up to 600 eV [26]. This energy range is particularly interesting for multiple purposes: It covers the important spectral range of the water window [27–31], and provides short enough wavelengths for wafer metrology on structures representative of current and future generations of nanotransistors in integrated-circuit manufacturing [32].

## 2. Overall system layout

Our OPCPA system comprises two main components: the pump laser and the OPCPA, and is schematically shown in Fig. 1. We begin by giving an overview of the entire system, and then proceed with a more in-depth discussion of the pump laser and OPCPA.

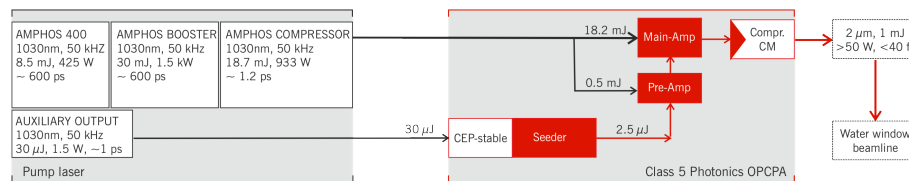


**Fig. 1.** Schematic overview of the pump laser / OPCPA system. The oscillator (integrated in main amplifier) is seeding both a main amplifier and an auxiliary output. The auxiliary output is independently compressed and used for seed generation in the OPCPA. The main amplifier is further amplified in the booster, and compressed in the main compressor. Subsequently, it is used for amplifying the seed in the OPCPA.

The pump laser is a high-power, picosecond Yb:YAG InnoSlab amplifier system (AMPHOS GmbH), and represents a prototype to this day. The amplifier system provides two main outputs: the main OPCPA pump (exiting the compressor of the Yb:InnoSlab pump laser) and an additional auxiliary output both at 1030 nm central wavelength. The main output at the compressor reaches a total of 933 W average power, with a pulse energy of 18.7 mJ at 50 kHz pulse repetition rate with a pulse duration of 1.2 ps FWHM. The auxiliary output is a small, separate amplifier that is seeded by the same oscillator/pre-amplifier as the main pump laser. It reaches an average power of 1.5 W with a pulse energy of 30  $\mu\text{J}$  at 50 kHz. The pulse duration is 900 fs.

The auxiliary output is used for stable OPCPA signal seed generation and can be operated independently from the main output. In this way, the OPCPA seed beam can be generated and operated without the high power output, which is used in two stages (preamplifier and V-shaped double-pass main amplifier) for amplification of the seed. This approach offers favorable long-term stability of the OPCPA signal generation and ease of use. The OPCPA pulses are subsequently compressed in a chirped-mirror compressor to 38 fs pulse duration.

### 3. InnoSlab pump laser

We now proceed to discuss the Yb:InnoSlab pump laser as well as the OPCPA in more detail.

The two independent outputs of the kW-class pump laser share the same front-end: a fiber-based oscillator, passively mode-locked by means of a semiconductor saturable absorber mirror (SESAM). The oscillator delivers seed pulses at a repetition rate of 39.8 MHz, with energy per pulse around 1 nJ at a central wavelength of 1030 nm. After the oscillator, the energy of the pulses is increased in a fiber amplifier. An acousto-optical modulator picks the pulses to be amplified in subsequent fiber amplifiers. This pulse picker allows operating the subsequent amplification over a wide range of repetition rates, in principle ranging from 10 kHz to 2 MHz. We have set the repetition rate to 50 kHz in the current configuration. The pulse picker is followed by a 50/50 beam splitter, for splitting the pre-amplified pulses with adjusted repetition rate into the auxiliary and main output. Both pulses from the two arms then seed two Yb:YAG pre-amplifiers in parallel. This increases the energy per pulse to around 30  $\mu\text{J}$  and 40  $\mu\text{J}$  for the aux and main pulse respectively.

The output of the low-energy auxiliary preamplifier is sent into a compact grating-based compressor, to compensate for the dispersion accumulated during the propagation in the pre-amplifiers. This compressed output is what is referred to as auxiliary output in this Letter. The specifications of the auxiliary output are summarized in Fig. 2(a)-c. Figure 2(a) shows an intensity autocorrelation trace of the pulses delivered by the auxiliary output, which has a FWHM of 1.4 ps, indicating a pulse duration of 900 fs for a  $\text{sech}^2$ -pulse. As these pulses generate the seed at 2  $\mu\text{m}$  in the OPCPA, outstanding long-term stability of the total output power of 1.5 W of the auxiliary output is desirable. Figure 2(b) shows an example of a stability measurement, which exhibits a standard deviation well below half a percent of the average power, over the course of six hours. The spectrum shown in Fig. 2(c) has a FWHM of 1.5 nm, indicating that the pulses are compressed to close to transform-limited duration.

The pulses coming from the high-energy preamplifier in the main amplifier are stretched in a fiber Bragg grating to a duration of about 500 ps to seed the next amplification stage. The beam is expanded and shaped in order to match the mode of the pump beam in the next amplification stage. The output of an array of high-brightness diodes at 938 nm is made into a homogeneous beam by means of a light-mixing duct, which is then used to pump the main InnoSlab crystal, where the seed propagates for 7 passes. The amplified pulses exceed 8.5 mJ, corresponding to 425 W.

A combination of a half-waveplate and a thin-film polarizer is used to set the pulse energy propagating to the booster amplification stage. In this stage, a second InnoSlab crystal is pumped by another array of diodes, in a double-pass configuration. The pulses are amplified to about 30 mJ, raising the average power to 1.5 kW. At the output of this stage, another combination of a half-waveplate and a thin-film polarizer is used to select the energy to be sent to the beam shaping and compression stage.

The amplification geometry of the InnoSlab crystals yields an elliptical mode, comprising higher-order, non-Gaussian components in the vertical direction. In order to improve the beam quality, the beam is spatially filtered. The filtered beam is then recollimated prior to the main grating-based compressor. The architecture of the compressor is based on two gratings, with a total of four bounces, leading to picosecond pulses. Figure 2(d) shows an intensity autocorrelation

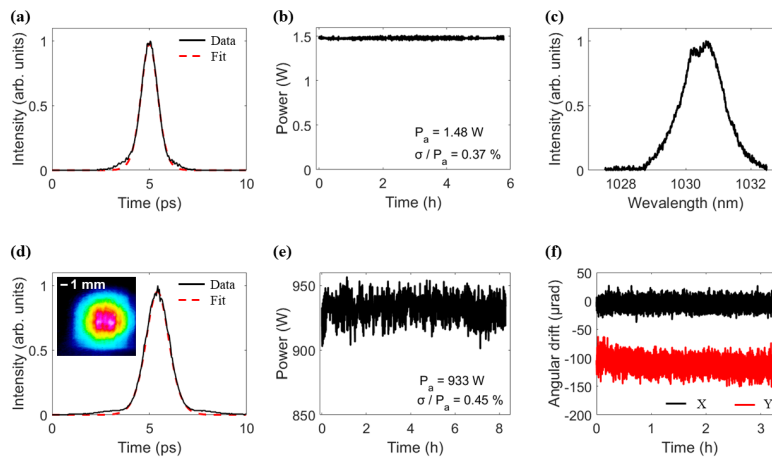


**Fig. 2.** Pulse characterization of the pump laser. Top row: auxiliary output. Bottom row: main output. (a) Intensity autocorrelation of the auxiliary pulses (solid black line) and fit (dashed red line,  $\text{sech}^2$ -convolution, assuming a hyperbolic secant squared temporal profile). (b) Long-term power stability of the auxiliary output. Average and relative standard deviation are reported in the plot. (c) Spectral intensity of the auxiliary output. (d) Intensity autocorrelation of the main pulses (solid black line) and fit (dashed red line,  $\text{sech}^2$ -convolution). The inset shows the beam profile of the main output. (e) Long-term power stability of the main output. (f) Long-term pointing stability of the main output, in the vertical (red line) and horizontal (black line) directions.

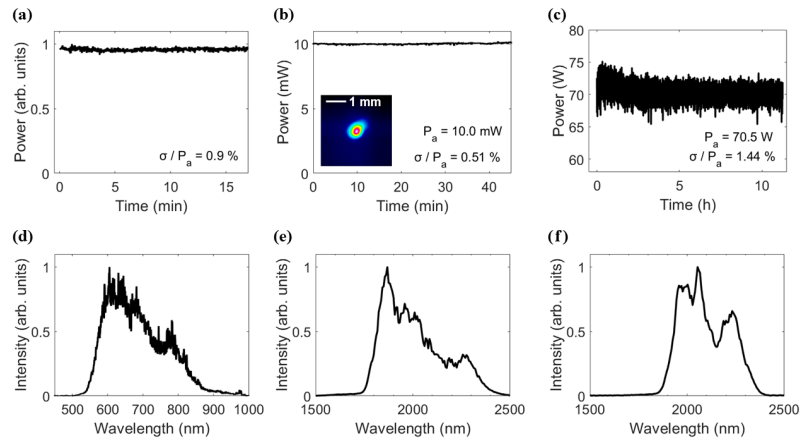
of the pulses delivered by the main output, with a FWHM of 1.9 ps, indicating pulses with a duration of 1.2 ps. The inset is a far-field beam profile, showing an almost Gaussian mode. The total transmission of the beam shaping and the compressor units is around 62%, leading to an output of 933 W after all losses, corresponding to 18.7 mJ per pulse. These 62% transmission are roughly comprised of a compressor transmission of 88%, and a scraping (beam shaping) transmission of 70%.

Figure 2(e) shows a long-term measurement of the power of the main output. It features a standard deviation of 0.45 % of the average power, over the course of eight hours. Given that a similar stability of the auxiliary output was measured in Fig. 2(b), stable operation of a subsequent OPCPA is feasible. Figure 2(f) shows the pointing stability of the main output, after a warm-up phase and with active pointing stabilization, again indicating good to excellent stability.

#### 4. Mid-infrared optical parametric chirped-pulse amplifier

In the following, we discuss the configuration of the OPCPA and first results. For the results shown in the following the pump laser was operated at 830 W. We set the power to this lower value of 830 W compared to the 933 W maximum output power to improve longevity of the diodes and incorporate a buffer for possible future diode degradation that would result in a lower output power.

We first discuss the seed generation, which is pumped by  $30\mu\text{J}$  (1.5 W) of the auxiliary output of the pump laser. In the OPCPA seed generation, the goal is to generate and amplify a broadband pulse at  $2\mu\text{m}$ . To this end, first, a portion of the auxiliary output is used for producing a broadband visible spectrum by white-light generation (WLG) in a bulk YAG crystal (10 mm). The power stability of this white-light spectrum is shown in Fig. 3(a), and its spectrum is depicted in Fig. 3(d).



**Fig. 3.** (a) Power stability of the white-light generation (WLG). (b) Power stability of difference frequency generation (seed). The inset shows a beam profile of the seed pulses. (c) Power stability of main amplifier OPCPA output. (d) WLG spectrum. (e) Spectrum of DFG (seed). (f) Spectrum of main amplifier at 70.5 W output power (as monitored in (c)).

The visible part of the WLG is used to pump a collinear difference frequency generation (DFG) stage, using  $\beta$ -barium borate crystal (BBO, 1 mm) with type-I phase-matching, seeded at a 1030 nm wavelength. The resulting broad-band idler pulse covers a spectral range from 1750–2500 nm. The power stability of this idler is shown in Fig. 3(b) and the spectrum is shown in Fig. 3(e). The pulse energy at this point is approximately 200 nJ.

The DFG is further amplified in a two-stage OPCPA, where the same 20  $\mu$ J of the auxiliary pump laser output pumps the amplification crystals. The amplified portion of the seed bandwidth can be adjusted by adapting the stretching factor of the 2  $\mu$ m signal with respect to the pump pulse duration. In the presented work, a bulk silicon stretcher is used to introduce positive dispersion. As a result, the target spectrum ranges from 1.85–2.3  $\mu$ m, with a pulse energy of 2.5  $\mu$ J.

The seeder is now amplified in the main optical amplification part, for which the power is supplied by the main output of the pump laser. This amplification consists of a 3-stage OPCPA, where the last two stages are a double-pass V-shaped amplifier. The pump in all stages is derived from the main output. The first stage (pre-amplifier) is pumped at 0.5 mJ and amplifies the pulses to 30  $\mu$ J. The second and third amplifier stages are pumped at 18.2 mJ. The same pump beam is used here for pumping both crystals, arranged in a V-shaped geometry. These amplification stages use BBO crystals (2 mm).

In the final V-shaped amplification, the second OPCPA stage is optimized for a gain factor of ca 250, achieving 40 W average power. The final third stage that uses the same pump achieves an additional amplification gain factor of 1.75, giving 70 W total power. Amplification factors of 1.5–2 are typical for amplification stages with a recycled pump. The amplified spectral bandwidth spans from 1900–2300 nm. The temporal delay drifts between main and auxiliary output, which affects the amplification of the seed, are measured and compensated using an optical cross-correlator in the OPCPA (not shown in the schematic).

Power stability and spectral intensity profile of the OPCPA output are shown in Fig. 3(c,f). These pulses still carry the same duration as the pump pulses (around 1 ps or slightly more.) Subsequently, the output is compressed. The whole approach of the system is a passive dispersion management approach, to reduce complexity. As the seeder provides a positively chirped output, a positive chirp is maintained through the entire system. This is finally compressed in a chirped mirror compressor consisting of 15 bounces on water-cooled mirror mounts. The



number of bounces was optimized for compression. The compressor output is 50 W, and the pulse characterization via second-harmonic generation (SHG) frequency-resolved optical gating (FROG) is shown in Fig. 4, showing an achieved pulse duration of 38 fs. While the transform limit of our pulses is in principle 28 fs, the duration of 38 fs was the best results currently achievable with our chirped mirror compressor, as there are remaining higher-order contributions to the phase as can be seen in Fig. 4(c).

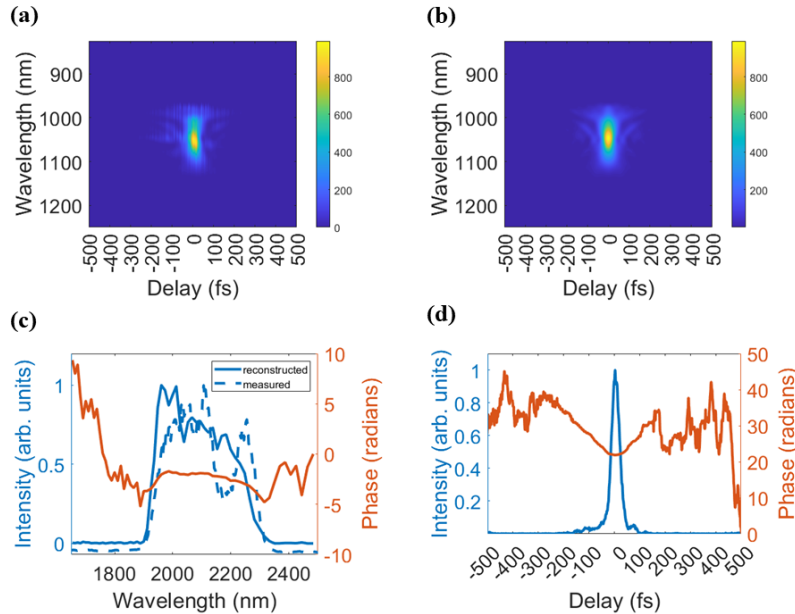


**Fig. 4.** Temporal characterization of compressed OPCPA output. (a) Measured SHG FROG trace. (b) Reconstructed SHG FROG trace. (c) Reconstructed spectrum (blue solid line) and spectral phase (red). The measured amplifier spectrum is also shown (blue dashed, same as in Fig. 3(f)). (d) Reconstructed temporal intensity profile of pulse (blue solid line) and temporal phase (red). The pulse duration is 38 fs.

## 5. Conclusion and outlook

In conclusion, we have demonstrated the development of an Yb:InnoSlab platform with kW-level average power as a pump source for a mid-infrared OPCPA. The pump laser produces 1-ps pulses with nearly 18.7 mJ at 50 kHz repetition rate, and good power and pointing stability. As such, the pump laser is ideally suited to drive a mid-infrared high-power optical parametric chirped-pulse amplifier system. First results from this mid-infrared OPCPA have been demonstrated including seed generation, amplification, and compression. We demonstrated 70 W generation of mid-infrared pulses at 2000 nm central wavelength, which resulted in 50 W average power at 38 fs.

Further optimization towards higher conversion efficiencies in the OPCPA are underway. In particular, further improvements of the mode profile and temporal contrast of the pump laser, as well as the choice of amplification crystals are possible knobs to turn. While BBO can amplify over a large bandwidth, other crystals such as KTA are known to provide superior efficiencies in parametric amplification.

This OPCPA will become an ideal source for generating soft-X-ray pulses at high average powers by high-harmonic generation, which will give access to generating energies approaching

600 eV. As such, the OPCPA will cover the important water window of soft-X-rays and thus enable new opportunities for spectroscopy and imaging in the SXR range.

**Funding.** HORIZON EUROPE European Research Council (101041819, ERC Starting grant “ANACONDA”); Nederlandse Organisatie voor Wetenschappelijk Onderzoek (18703, Open Technology Programme).

**Acknowledgments.** We thank Amphos GmbH for setting up the pump laser and commenting on the manuscript. We thank all ARCNL support departments (mechanical design and workshop, electronic engineering and software engineering) for continuous support.

Part of this work was conducted at the Advanced Research Center for Nanolithography, a public-private partnership between the University of Amsterdam (UvA), Vrije Universiteit Amsterdam (VU), Rijksuniversiteit Groningen (RUG), the Netherlands Organization for Scientific Research (NWO), and the semiconductor equipment manufacturer ASML and was (partly) financed by 'Toeslag voor Topconsortia voor Kennis en Innovatie (TKI)' from the Dutch Ministry of Economic Affairs and Climate Policy.

**Disclosures.** Class 5 Photonics is a commercial company that sells OPCPA's. Besides, the authors declare no conflicts of interest.

**Data availability.** Data underlying the results presented in this paper are not publicly available at this time but may be obtained from the authors upon reasonable request.

## References

1. O. O. Versolato, J. Sheil, S. Witte, *et al.*, “Microdroplet-tin plasma sources of EUV radiation driven by solid-state-lasers (Topical Review),” *J. Opt.* **24**(5), 054014 (2022).
2. R. Schupp, L. Behnke, J. Sheil, *et al.*, “Characterization of 1-and 2- $\mu$  m-wavelength laser-produced microdroplet-tin plasma for generating extreme-ultraviolet light,” *Phys. Rev. Res.* **3**(1), 013294 (2021).
3. P. Zeitoun, G. Faivre, S. Sebban, *et al.*, “A high-intensity highly coherent soft x-ray femtosecond laser seeded by a high harmonic beam,” *Nature* **431**(7007), 426–429 (2004).
4. Y. Wang, E. Granados, F. Pedaci, *et al.*, “Phase-coherent, injection-seeded, table-top soft-x-ray lasers at 18.9 nm and 13.9 nm,” *Nat. Photonics* **2**(2), 94–98 (2008).
5. S. Witte and K. S. E. Eikema, “Ultrafast optical parametric chirped-pulse amplification,” *IEEE J. Sel. Top. Quantum Electron.* **18**(1), 296–307 (2012).
6. G. Cerullo and S. De Silvestri, “Ultrafast optical parametric amplifiers,” *Rev. Sci. Instrum.* **74**(1), 1–18 (2003).
7. B. E. Schmidt, N. Thiré, M. Boivin, *et al.*, “Frequency domain optical parametric amplification,” *Nat. Commun.* **5**(1), 3643 (2014).
8. M. Schulz, R. Riedel, A. Willner, *et al.*, “Yb:YAG Innoslab amplifier: efficient high repetition rate subpicosecond pumping system for optical parametric chirped pulse amplification,” *Opt. Lett.* **36**(13), 2456–2458 (2011).
9. B. E. Schmidt, A. Hage, T. Mans, *et al.*, “Highly stable, 54mJ Yb-InnoSlab laser platform at 0.5kW average power,” *Opt. Express* **25**(15), 17549–17555 (2017).
10. J. Novák, J. T. Green, T. Metzger, *et al.*, “Thin disk amplifier-based 40 mJ, 1 kHz, picosecond laser at 515 nm,” *Opt. Express* **24**(6), 5728–5733 (2016).
11. J.-P. Negel, A. Loescher, A. Voss, *et al.*, “Ultrafast thin-disk multipass laser amplifier delivering 1.4 kW (4.7 mJ, 1030 nm) average power converted to 820 W at 515 nm and 234 W at 343 nm,” *Opt. Express* **23**(16), 21064–21077 (2015).
12. C.-L. Chang, P. Krogen, K.-H. Hong, *et al.*, “High-energy, kHz, picosecond hybrid Yb-doped chirped-pulse amplifier,” *Opt. Express* **23**(8), 10132–10144 (2015).
13. P. Russbuehlt, D. Hoffmann, M. Höfer, *et al.*, “Innoslab amplifiers,” *IEEE J. Sel. Top. Quantum Electron.* **21**(1), 447–463 (2015).
14. C. Schnitzler, T. Mans, J. Dolkemeyer, *et al.*, “High power, high energy, and high flexibility: powerful ultrafast lasers based on InnoSlab technology,” *Proc. SPIE* **10911**, 1091103 (2019).
15. T. G. Mans, M. Blecher, A. Hage, *et al.*, “High average power 10GW laser sources,” *Proc. SPIE* **11664**, 1166400 (2021).
16. T. Golz, J. H. Buß, M. Schulz, *et al.*, “High power CEP-stable OPCPA at 800nm,” *Proc. SPIE* **11259**, 112591L (2020).
17. J. H. Buss, I. Grguraš, S. Starosielec, *et al.*, “High-power OPCPAs at 1450–2400 nm wavelength,” *Proc. SPIE* **11670**, 116700Y (2021).
18. M. F. Seeger, D. Kammerer, J. Blöchl, *et al.*, “49 W carrier-envelope-phase-stable few-cycle 2.1  $\mu$ m OPCPA at 10 kHz,” *Opt. Express* **31**(15), 24821–24834 (2023).
19. T. Feng, A. Heilmann, M. Bock, *et al.*, “27 W 2.1  $\mu$ m OPCPA system for coherent soft X-ray generation operating at 10 kHz,” *Opt. Express* **28**(6), 8724–8733 (2020).
20. Y. Deng, A. Schwarz, H. Fattahi, *et al.*, “Carrier-envelope-phase-stable, 1.2 mJ, 1.5 cycle laser pulses at 2.1  $\mu$ m,” *Opt. Lett.* **37**(23), 4973–4975 (2012).
21. M. K. R. Windeler, K. Mecseki, A. Miahnahri, *et al.*, “100 W high-repetition-rate near-infrared optical parametric chirped pulse amplifier,” *Opt. Lett.* **44**(17), 4287–4290 (2019).
22. N. Thiré, R. Maksimenka, B. Kiss, *et al.*, “Highly stable, 15 W, few-cycle, 65 mrad CEP-noise mid-IR OPCPA for statistical physics,” *Opt. Express* **26**(21), 26907–26915 (2018).

23. M. Bridger, O. A. Naranjo-Montoya, A. Tarasevitch, *et al.*, “Towards high power broad-band OPCPA at 3000 nm,” *Opt. Express* **27**(22), 31330–31337 (2019).
24. M. Mero, Z. Heiner, V. Petrov, *et al.*, “43 W, 1.55  $\mu\text{m}$  and 12.5 W, 3.1  $\mu\text{m}$  dual-beam, sub-10 cycle, 100 kHz optical parametric chirped pulse amplifier,” *Opt. Lett.* **43**(21), 5246–5249 (2018).
25. P. M. Kraus and H. J. Wörner, “Perspectives of attosecond spectroscopy for the understanding of fundamental electron correlations,” *Angewandte Chemie Int. Ed.* **57**(19), 5228–5247 (2018).
26. P. M. Kraus, M. Zürch, S. K. Cushing, *et al.*, “The ultrafast X-ray spectroscopic revolution in chemical dynamics,” *Nat. Rev. Chem.* **2**(6), 82–94 (2018).
27. T. Popmintchev, M.-C. Chen, D. Popmintchev, *et al.*, “Bright Coherent Ultrahigh Harmonics in the keV X-ray Regime from Mid-Infrared Femtosecond Lasers,” *Science* **336**(6086), 1287–1291 (2012).
28. S. L. Cousin, F. Silva, S. Teichmann, *et al.*, “High-flux table-top soft x-ray source driven by sub-2-cycle, CEP stable, 1.85- $\mu\text{m}$  1-kHz pulses for carbon K-edge spectroscopy,” *Opt. Lett.* **39**(18), 5383–5386 (2014).
29. A. S. Johnson, D. R. Austin, D. A. Wood, *et al.*, “High-flux soft x-ray harmonic generation from ionization-shaped few-cycle laser pulses,” *Sci. Adv.* **4**(5), eaar3761 (2018).
30. J. Pupeikis, P.-A. Chevreauil, N. Bigler, *et al.*, “Water window soft x-ray source enabled by a 25 W few-cycle 2.2  $\mu\text{m}$  OPCPA at 100 kHz,” *Optica* **7**(2), 168–171 (2020).
31. L. Barreau, A. D. Ross, S. Garg, *et al.*, “Efficient table-top dual-wavelength beamline for ultrafast transient absorption spectroscopy in the soft X-ray region,” *Sci. Rep.* **10**(1), 5773 (2020).
32. C. Porter, T. Coenen, N. Geypen, *et al.*, “Soft x-ray: novel metrology for 3D profilometry and device pitch overlay,” *Proc. SPIE* **12496**, 124961I (2023).